Carbohydrate Polymers 87 (2012) 1354–1362

Contents lists available at SciVerse ScienceDirect

Carbohydrate Polymers

journal homepage: www.elsevier.com/locate/carbpol

Hydrogels and electrospun nanofibrous scaffolds of N-methylene phosphonic chitosan as bioinspired osteoconductive materials for bone grafting

Pallab Datta, Santanu Dhara*, Jyotirmoy Chatterjee

School of Medical Science and Technology, Indian Institute of Technology Kharagpur, Kharagpur, West Bengal 721302, India

ARTICLE INFO

Article history:
Received 30 July 2011
Received in revised form 4 September 2011
Accepted 7 September 2011
Available online 14 September 2011

Keywords:
α-Amino phosphorylation
Mineralization
Gelation
Crosslinkers
Electrospinning parameters
Osteoinduction

ABSTRACT

In this work, N-methylene phosphonic chitosan (NMPC) based hydrogels and electrospun nanofibrous scaffolds are reported with objective to obtain osteoconductive and osteoinductive matrixes for bone grafting applications. NMPC, a phosphorylated derivative of chitosan, is known to mimic the function of non collagenous phosphoproteins in providing nucleation sites for biomineralization. NMPC hydrogels were prepared by crosslinking between NMPC and genipin. A detailed investigation of physicochemical properties of NMPC solutions is also carried out in order to obtain beads free nanofibers. Both NMPC gels and nanofibers were further evaluated for their biomineralization potential and biocompatibility with human osteoblast like cells. Results indicated that hydrogels and nanofibrous scaffolds NMPC are biocompatible and significantly osteoinductive compared to tissue culture plate controls. However, cells seeded on nanofibrous scaffolds exhibited greater proliferation measured by MTT assay, and higher expression of early markers for osteogenic differentiation proving the superior applicability of nanofibrous scaffolds for bone grafting applications.

1. Introduction

Bone is an organic–inorganic hybrid tissue in which the major organic component collagen nano-fibrils is mineralized by apatite nano-crystals (Stevens, 2008). This assembly of organic fiber–inorganic crystals is principally responsible for mechanical properties of bone. Most of the bone grafts fail due to their inability to match the mechanical properties of native bone, form a strong bond and integrate completely (osseointegration) with bone tissue at the injury site (Song, Malathong, & Bertozzi, 2005). The process of osseointegration is determined by presence of a osteoconductive matrix, osteoinductive factors in the milieu and delivery of osteogenic cells at the site. In this respect, it is now known that the presence of calcium-phosphate layers on the grafted materials can enhance the osteoconductivity of a matrix which amongst the three processes is the first step towards bone integration (Cornell, 1999). Though hybrid composites with various calcium phosphates is an approach often employed to enhance osteoconductivity, *in situ* generation of ordered fiber–crystal arrays similar to *in vivo* biomineralization phenomenon presents a promising alternative (Uchino, Kamitakahara, Otsuka, & Ohtsuki, 2010).

Chitosan, due to its structural similarity to the glycosaminoglycan/proteoglycan molecules found in bone extracellular matrix, is used as an analogous material for structural regeneration (Kim et al., 2008). The structural similarities pertain to the repeating saccharide units. However, as present endeavors of tissue engineering moves from mere structural to functional restoration, the presence of reactive amino and hydroxyl groups in the repeating glucosidic units of chitosan is gaining more attention for chemical modifications and make the polymer amenable to yield biofunctional materials (Alves & Mano, 2008).

Though chitosan is shown to posses bone formation properties, scope for functionalization of the polymer exists (Seol et al., 2004). Grafting of anionic groups on polymer backbone is postulated to address many shortcomings of chitosan as it provides a negatively charged surface for relevant protein adsorption, *in situ* nucleation sites for calcium-phosphate mineralization and enhancement of cellular adhesion (Jung, Na, & Kim, 2007; Kretlow & Mikos, 2007). Amongst various anioinic groups, phosphorylation offers a bioinspired approach as it is also an essential biochemical modification of matrix proteins engaged in mineralization and bone formation *in vivo* (George & Veis, 2008). Moreover, ion-exchange properties of phosphate groups provide adequate functionalities for specific binding of bioactive signaling molecules (Ilyina, Varlamov, Tikhonov, Yamskov, & Davankov, 1994; Sugihara, Imamura, Yanase, Yamada, & Imoto, 1982), an approach now gaining attention in regenerative medicine, in contrast to the convention of growth factors delivery through diffusion (Orban, Marra, & Hollinger,

* Corresponding author. Tel.: +91 3222 282306; fax: +91 3222 282221.
E-mail addresses: contactpallab@gmail.com (P. Datta), sdhara@smst.iitkgp.ernet.in (S. Dhara), jchatterjee@smst.iitkgp.ernet.in (J. Chatterjee).

0144-8617/$ – see front matter © 2011 Elsevier Ltd. All rights reserved.
doi:10.1016/j.carbpol.2011.09.023

2002). Thus many phosphorylated derivatives of chitosan have been investigated for several biomedical applications. For example, Amaral, Granja, and Barbosa (2005) have performed surface phosphorylation of chitosan films (Amaral et al., 2005), Zhu, Wang, Cui, Feng, and Groot (2003) reported the ability of a phosphorylated chitosan to induce osteoblast differentiation (Zhu et al., 2003) and López-Pérez, da Silva, Serra, Pashkuleva, and Reis (2010) have found improved osteoblast response on chitosan membranes surface phosphorylated by vinyl phosphoric acid (López-Pérez et al., 2010). Yin et al. (2004) were the first to explore feasibility of freeze dried NMPC for enhancing mineralization potential of chitosan scaffolds (Yin et al., 2004). Studies by Pramanik et al. (2009) and Tang et al. (2011) also demonstrated the effect of various phosphorylated chitosan in inducing osteogenic differentiation (Pramanik et al., 2009; Tang et al., 2011). Further, Ramos et al. (2006) furnished a method of synthesizing crosslinked NMPC hydrogels by polyethylene glycol aldehyde (Ramos et al., 2006). In addition, some recent publications strongly suggest ability of phosphorylated chitosan to act as templated biomimetic analogues of non collagenous proteins in mediating bone mineralization (Xu, Neoh, Lin, & Kishen, 2011). Notwithstanding the obvious advantages of phosphorylated chitosan for osteoconductive bone grafting, to the best of our knowledge no literature is available on NMPC gels and nanofibers suitable for real situation biomedical applications.

The aim of present study is to develop hydrogels and electrospun nanofibers of a phosphorylated derivative of chitosan, N-methylene phosphonic chitosan (NMPC) as biocompatible material for bone graft. Genipin, a natural product with one of the least toxicity amongst those used for curing chitosan, is used as an crosslinking agent for fabrication of NMPC hydrogels (Muzzarelli, 2009). The potential of nanofibers in bone tissue engineering is well known in the state of the art (Chakraborty, Liao, Adler, & Leong, 2009). *In situ* mineralization on both hydrogels and nanofibers were compared and their biocompatibility evaluated by observing response of human pre-osteoblast like MG 63 cell lines.

2. Materials and methods

2.1. Synthesis of N-methylene phosphonic chitosan

Chitosan was phosphorylated by a method well cited in the literature (Ramos et al., 2006). Briefly, 3% (w/v) chitosan (Marine Chemicals, Cochin India, Grade <90% deacetylated) solution in 0.5 M glacial acetic acid was charged in a three necked round bottom flask (RBF). Phosphorous acid (one part by weight) was added drop-wise with continuous stirring for an hour at room temperature. After addition, temperature of RBF was raised to 70 °C and a reflux condenser was attached. This was followed by gradual addition of 6 ml formaldehyde solution to the RBF for 1 h. Heating was protracted at the same temperature for 14 h. After the reaction, the pale yellow solution was cooled down to room temperature and the product was precipitated in excess ethanol. The product was solubilized in water, reprecipitated and washed with ethanol, the process repeated five times to remove any unreacted acids and formaldehyde. Finally, the product was vacuum dried at 50 °C. Elemental analysis was performed in an EDX spectrophotometer (Inca PentaFET-3, Oxford Instruments, UK) on the uncoated sample to ensure presence of phosphate in the modified polymer.

2.2. NMR spectroscopy

Dried product was dissolved in D_2O at concentration of 50 mg/ml and ^{13}C NMR spectra was recorded on an AVANCE DAX-400 (Bruker, Sweden) 400 MHz NMR spectrometer.

2.3. Gelation study of NMPC with genipin

To develop biocompatible hydrogels, gelation of NMPC with genipin was first investigated by inverted vial method. Solutions of different genipin (Challenge Bioproducts, Taiwan) concentrations (0.5–1.5%, w/v) were added to 8% solution of NMPC in equal volumes and stirred well for 5 min. Vials were then incubated at 37 °C and inverted every 15 min to observe flow behavior. In the experiment, solution state was defined as flowing liquid and gelation was asserted when no flow occurred after the vial was inverted and held for 1 min.

Malvern-Bohlin CVO rheometer with parallel plate (gap 100 μm) geometry was employed for rheological characterization and study of gelation kinetics of NPMC–genipin gel by oscillatory stress, and time sweep measurements. Controlled stress amplitude sweep at constant frequency (1 Hz) were performed on 24 h cured hydrogels to determine the linear viscoelastic region (LVR) property. Afterwards, time sweep at 5 Pa stress was performed to monitor *in situ* gelation behavior of the selected genipin solution, enabling the evaluation of elastic storage modulus (G') and viscous loss modulus (G'') with time. Time point at which G' intersected G'' was assumed to be the gelation time and correlated with inverted vial results. All experiments were performed at 37 °C.

2.4. Physico-chemical properties of NMPC

Weighed polymer samples were placed in deionized water to allow initial swelling followed by mechanical stirring for 2 days at room temperature. Homogenous solution was ascertained by visual inspection against a light source and flow of polymer solution against the walls of test tube. If required, the solutions were de-aired by mild centrifugation. The solutions were filtered ensuring that no gelatinous mass is retained on the filtrand, and if found any, the batch was discarded and solutions were prepared afresh. Polymer blends of NMPC and PVA were prepared by appropriately mixing individual polymer solutions and stirring for further 2 days for homogenous distribution of each polymer phase. pH and conductivity were measured for samples synthesized in three batches by Cyberscan PC 510 (Eutech Instruments, Singapore). Surface tension was measured on tensiometer with platinum plate (DCAT 100, Dataphysics GmBH, Germany) and the Bohlin CVO D100 (Malvern, UK) rheometer was used for viscosity measurements with a CP 4/40 geometry (gap 150 μm) at 25 °C. Temperature was maintained with help of Peltier controlled heating element. For all measurements, an equilibrium time of 120 s was set before start of a rheology test.

2.5. Optimization of electrospinning parameters

The electrospinning set up consisted of a high voltage DC power supply (Glassman, Japan), a blunted 26 gauge needle, syringe pump with variable flow rate, (KD Scientific, USA), and an electrically grounded copper collector covered with aluminum foil. Different polymer solutions were fed into a syringe connected to the needle tip. Feasibility of electrospinning was studied for different solutions at applied voltages of 12–18 kV, 0.5–15 μl/min solution flow rate, and tip-collector distances of 5–15 cm. As spun deposits were gold coated (Polaron, UK) and inspected under SEM (EVO 60, Carl Zeiss SMT, Germany) and EDX. Once obtained, samples with beads-free nanofibrous architectures were crosslinked in 40 mM glutaraldehyde–0.5% genipin solution for 3 h and thoroughly washed to remove any free glutaraldehyde from surfaces.

2.6. FTIR spectra

FTIR spectroscopy of chitosan, N methylene phosphorylated chitosan, and genipin crosslinked NMPC, were performed after finely

grinding a portion of each sample with KBr (in a mass ratio of 1:50) on a Perkin Elmer Spectrophotometer analyzed by spectrum GX software. FTIR spectrum of electrospun nanofibers were obtained by using a horizontal ATR attachment.

2.7. In vitro mineralization

Simulated body fluid (SBF) solution was prepared as per the formula of Kokubo and Takadama (Kokubo & Takadama, 2006). Both genipin crosslinked hydrogels and ethanol treated nanofibrous scaffolds (15 mm × 15 mm × 1 mm) were immersed in 1× SBF solution in culture dishes. Culture dishes were incubated in water bath (Sunbim, India) at 37 ± 0.5 °C. SBF solution was replaced every day. After 3 days of incubation, samples were taken out of the solution and washed three times with deionized water to remove the loosely bound impurities. Samples were air dried, sputter coated with gold and examined under SEM for morphology and mineral deposition. For qualitative compositional analysis by EDX, gold coating was eliminated.

2.8. Cell culture experiments

MG 63 cells, which exhibit a number of characteristic features similar to osteoblasts, were cultured in standard MG 63 media–DMEM media supplemented with 3.7% sodium bicarbonate, 10% FBS, 2 mM sodium pyruvate, 1 mM L-glutamine and 1% antibiotic antimyotic solution (All Himedia, India) in standard conditions of 37 °C, 95% humidity and 5% CO_2 (Heracell 150i, Thermo, USA). Cells were detached from culture flasks by EDTA–trypsin treatment for 5 min and centrifuged at 1200 rpm for further 5 min. Cell count for seeding density was performed by Countess (Invitrogen, USA).

2.9. Cellular viability

Samples of identical dimensions were sterilized in 70% ethanol and pre-soaked in medium overnight before cells were seeded at density of 4×10^5 cells/scaffold. Culture media was changed every 2 days. Cellular viability on various scaffolds was assessed using the MTT dye reduction technique. At the end of 12 h, 3 days, and 7 days, culture medium was discarded by pipetting, each well washed with PBS thrice and incubated with 200 μl of 5 mg/ml MTT solution (Sigma) at 37 °C for 4 h. The insoluble formazan crystals formed were allowed to dissolve in DMSO for 30 min. A standard curve was prepared from suspension of a known number of cells determined by Countess. Absorbance was read in 96-well plates on a microplate reader at 570 nm on Platescreen (RMS, Chandigarh, India).

2.10. Microscopy observation of cellular responses

Fluorescent staining of cells was performed by rhodamine–phalloidin and Hoechst dyes (Molecular Probes, Cat. No. R415, H21491) following manufacturer's instructions. Images were acquired by AxioVision microscope (Carl Zeiss, Germany). For SEM imaging, scaffolds were carefully removed from the culture dishes, washed with PBS thrice, fixed in 3.7% glutaraldehyde solution for 1 h, and dried with gradient ethanol/water for further 1 h. Nanofiber-cell constructs were sputter coated with gold to a thickness of 10–20 nm and observed by SEM. Images were grabbed at magnifications giving best clarity and resolution for each.

2.11. ALP activity and calcium deposition by MG63 cells

For cellular differentiation studies, ALP assay was performed according to the procedure reported by Lennon and Caplan (Lennon & Caplan, 2006). For all the scaffolds an acellular blank reading after incubation with PNPP was also obtained and subtracted from the cell-scaffold readings. The samples were stained and dye was extracted by a well cited literature method and absorbance taken at 570 nm to quantify the calcium deposition by MG 63 cells (Madurantakam et al., 2009).

2.12. Statistical analysis

Results are presented as mean ± SD. Comparisons were made using Origin Pro8 software for paired t tests and significant difference was asserted at 95% confidence intervals ($p < 0.05$).

3. Results and discussion

3.1. Synthesis and chemical identification of NMPC

Chitosan was modified by a Mannich type reaction proposed by Moedritzer and Irani for preparation of α-aminomethyl phosphonic acids. Orthophosphorous acid was used as the phosphorylating agent, while formaldehyde was used to prevent reaction in the direction of formation of phosphites (phosphorylation of the hydroxyl groups in chitosan) and preferentially yield NMPC (Matevosyan, Yukha, & Zavlin, 2003; Moedritzer & Irani, 1966). Chitosan was phosphorylated to yield NMPC since amongst other derivatives, NMPC is known to have high chelation ability for Ca^{2+} (Nishi et al., 1986), high gene delivery efficacy (Zhu et al., 2010), and filmogenic (Ramos, Rodríguez, Agulló, Rodríguez, & Heras, 2002) properties. However, fabrication of biocompatible NMPC based scaffolds and their cellular responses are not yet reported. To obtain a product with controlled degree of substitution, reaction conditions were optimized by adding 1:1:1 parts by weight of chitosan, phosphorous acid and formaldehyde in that order with reflux time of 14 h at 70 °C. The product obtained had the elemental composition of C (27.1%), N (6.79%), O (57.87%), P (8.24%), and was pale yellow in color. The product was soluble in water as well as acetic acid and decomposition range of product was found between 160 °C and 210 °C, which was lower than the starting material (230–245 °C).

To ascertain the chemical identity of product after phosphorylation reaction, ^{13}C NMR spectrum was obtained in D_2O and along with the schematic depiction of chemical reaction is shown in Fig. 1A and B. Chemical shift values of product were as follows: NMPC ^{13}C NMR δ 97.3 (anomeric C1), δ 55.64 (C2), δ 70.32 (C3), δ 76.08 (C4), δ 74.62 (C5), δ 59.75 (C6) which were typical for the chitosan polysaccharide. A doublet at δ 55.3 and multiplet at δ 38.16–37.31 ($-CH_2-P$) were also present indicating presence of methylene phosphonic groups in chitosan backbone. Chemical shift values obtained closely matches the values reported in the literature (Lebouc, Dez, & Madec, 2005). Out of the principal area of interest, peaks were found corresponding to the carbonyl and methyl groups of the N-acetyl-D-glucosamine units of chitosan at δ 174.91 and δ 21.98 ppm, respectively. In the spectrum, all the peaks are well resolved, distinct and attributed to all the six carbon atoms of pyranose ring. Absence of any other additional peaks corresponding to aldehydic and ketonic groups ruled out possibilities of any decomposition induced in the pyranose ring due to reaction conditions. NMR investigations along with EDX spectral analysis allowed defining the chemical composition of the synthesized product which is essential to control and assess the effects on cell culture studies.

3.2. Gelation of NMPC–genipin

For the development of biocompatible hydrogel scaffolds, gelation induced by crosslinking reaction of NMPC with a non

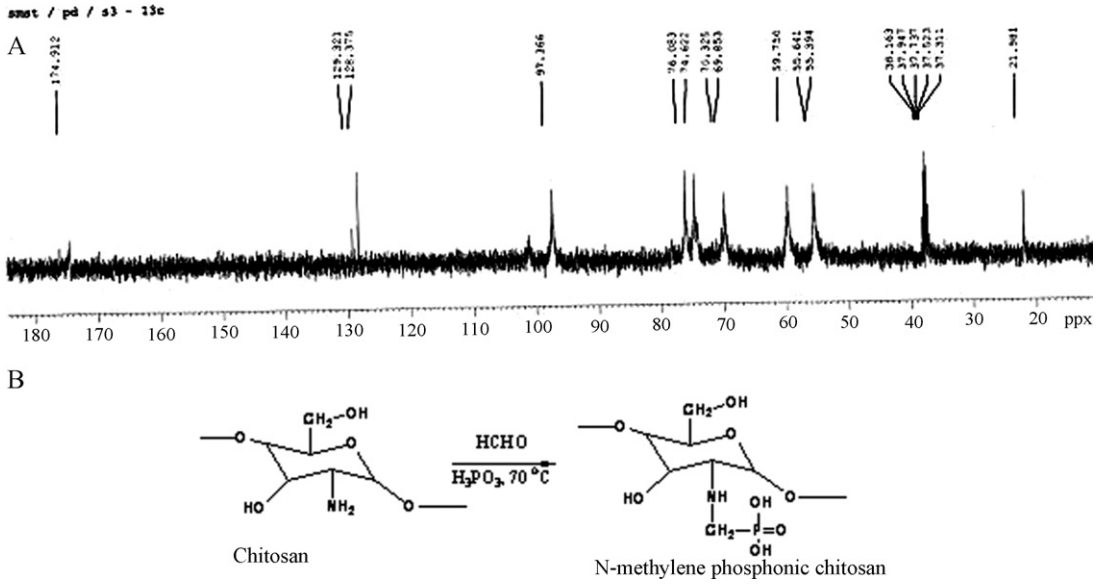

Fig. 1. (A) ^{13}C NMR spectrum of N-methylene phosphonic chitosan (NMPC) in D_2O (50 mg/ml) and (B) the reaction scheme adopted to obtain NMPC from chitosan.

toxic agent – genipin was optimized by inverted vial method and validated by oscillatory rheology (Moura, Figueiredo, & Gil, 2007). Inverted vial results revealed that gelation occurred at all the concentrations of genipin studied, but the time of gelation decreased with increase in genipin concentration for same concentration of NMPC. For example at 0.25% genipin concentration, the polymer solution took 5 h to form a gel at 37 °C, 0.33% genipin concentration took 3.75 h, 0.5% took 3.25 h to form NMPC gel while for 0.75% genipin, the time recorded was 2.45 h. The reaction was accompanied by transition in solution color from transparent to light yellow to deep blue. For accurate determination of gel properties, gel formation was further followed by oscillatory rheometry. Hydrogels formed by addition of different genipin concentrations after 24 h of reaction were subjected to stress amplitude sweep measurement for gel strengths. In Fig. 2A, concentration dependence of gel strength was evident from the elastic modulus (G') values which were 185.45, 869.48, 1471.33 and 1595.50 Pa for 0.25%, 0.33%, 0.50% and 0.75% genipin concentrations, respectively. The critical stress was found to be similar for gels formed with 0.33% and 0.50% and 0.75% of genipin. For the critical stress in 0.25% genipin, while the G'' increased at the same stress as for other concentrations tested, there was a slight delay in decrease in G' values. Based on these observations, we chose 0.75% genipin concentration to fabricate hydrogels for further evaluation. Fig. 2B shows the outcome of time sweep experiment of *in situ* crosslinking of 0.75% (w/v) genipin with 4% (w/v) NMPC which helps in determining accurate gelation time. At the start of experiment, when curing of polymer network has not taken place, G'' remained higher than G' indicating liquid like viscous flow. As the crosslinking progressed, the liquid like state was converted to a solid like state with accompanied response of the structure changing from predominantly viscous to elastic like. Along with formation of crosslinks, both G' and G'' showed a gradual increase. However, the rate at which G' increased was much higher than G'' indicating the process of gelation is taking place. The cross over point was located at 3 h after start of reaction, and the phase angle of the system at this point was found to be 49°. The gelation time, 3 h obtained by the oscillatory rheometry was found to be in close proximity to the 2.45 h observed by the inverted vial method. Examination of gelation time by both the methods – though the results are in close proximity to each other, enables us to under-

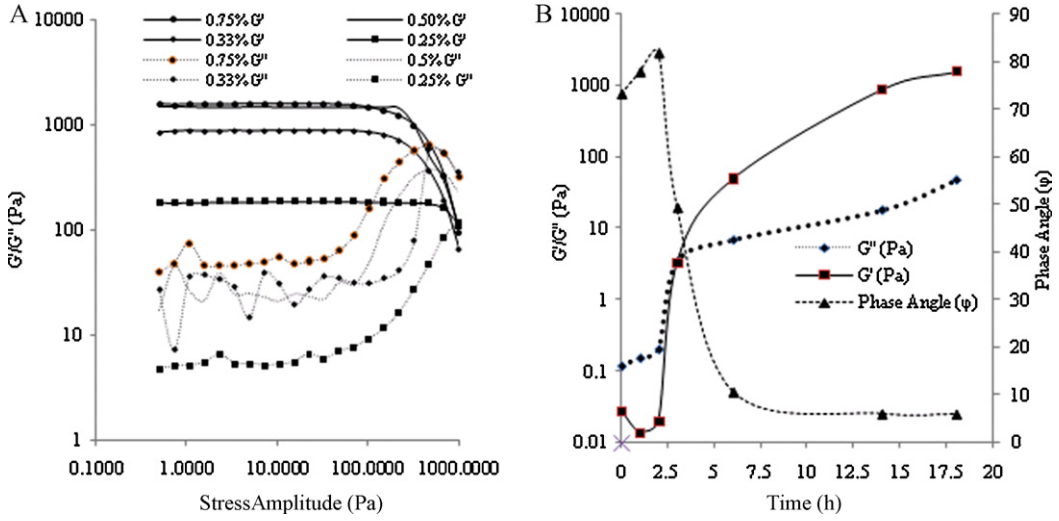

Fig. 2. (A) Gel strengths of hydrogels formed by crosslinking of NMPC by different concentration of genipin at 1 Hz frequency, (B) monitoring the gelation kinetics of NMPC–genipin gels (0.5%) by recording G', G'' and Φ at different time points at constant frquency of 1 Hz and stress of 20 Pa.

stand that though cross linking reaction is still progressing after the cross over point, the no visual change in flow behavior is taking place.

3.3. Optimization of electrospun nanofibers

In successful electrospinning, optimal solution parameters like surface tension, conductivity and viscosity form a delicate balance of forces to enable formation of submicron scale continuous fibers. In case of chitosan, the balance is achieved either in very strongly acidic organic solvents having low surface tension, having ability to diminish hydro-colloid behavior through charge shielding, like trifluoroacetic acid, 90% acetic acid etc. or in presence of additives such as polyethelyne oxide and Triton X. Rigid crystallinity and strong intermolecular hydrogen bonds manifested as high viscosity of chitosan solutions are deemed to be responsible for preventing formation of submicron fibers from aqueous solvents during electrospinning (Bhattarai, Edmondson, Veiseh, Matsen, & Zhang, 2005). XRD pattern of NMPC showed a marked reduction in the crystallinity compared to chitosan as seen in Fig. 3A and NMPC was water soluble. Despite this fact, NMPC solutions failed to electrospun at the concentrations tested (2–8%, w/w) and demonstrated splashing under applied electric field (Fig. 4A).

Investigation of physicochemical properties of aqueous NMPC (Table 1) revealed high surface tensions (66.16 ± 0.13 mN/m) indicating that grafting of hydrophilic phosphonic groups are not able to alter surface activity compared to chitosan. Highly concentrated and viscous solutions of NMPC (8%) in 1 M acetic acid had relatively low surface tension (58 mN/m) but produced agglomerated nanoparticles (Fig. 4B) during electrospinning. In attempt to further reduce surface tension, Triton X (1%) was added to the solutions for electrospinning. Addition of Triton X successfully decreased the surface tension to 40.69 mN/m, however the as spun sheets (Fig. 4C), demonstrated a predominantly beaded structure with traces of fibers. This may be due to the fact that addition of surfactant also resulted in drastic decline in the viscosity of NMPC solution to 0.085 Pa s from 1.02 Pa s of 8% (w/v) phosphorylated polymer solution in acetic acid medium. Further, 1 M NaCl was added as a solute in order to allow more surface charges so that repulsive forces in the polymer solution can yield uniform nanofibers. Compared to the NMPC–acetic acid–Triton X mixture, no advantage was achieved in the fiber morphology after addition of salt (Fig. 4D). It was noted that solution conductivity of the system is exceeding 4 mS/cm and possibly causing jet instabilities so that electrospinning from solutions of very high conductivities were also unsuccessful to yield beads free nanofibers (Angammana & Jayaram, 2008). All the above trials and errors and the morphologies obtained thereof indicated the need for decreasing the solution conductivity, surface tension and increasing the viscosity of NMPC solutions to an optimum level to attain beads-free and defect free fibers. Polyvinyl alcohol was chosen as the additive here due mostly to its ability to enhance electrospinnability of difficult-to-electrospin materials, proven biocompatibility and ease of crosslinking. The addition of PVA in proportion of 1:4 to NMPC solution (total polymer 8%, w/w) illustrated the role of PVA in influencing the electrospinning process. A beads-on-string nanofibrous morphology was seen in the SEM images of as spun deposits as shown in Fig. 4E. When PVA ratio corresponding to NMPC was increased to 1:1.5 (see Table 1) by weight (Fig. 4F), completely beads free and defects free fibrous morphology was obtained. PVA is known to decrease the molecular associations and viscosity of chitosan solutions without loss of entanglements thereby facilitating chitosan electrospinning (Ohkawa, Cha, Kim, Nishida, & Yamamoto, 2004). However, in case of NMPC, where the molecular weight and viscosity is inherently

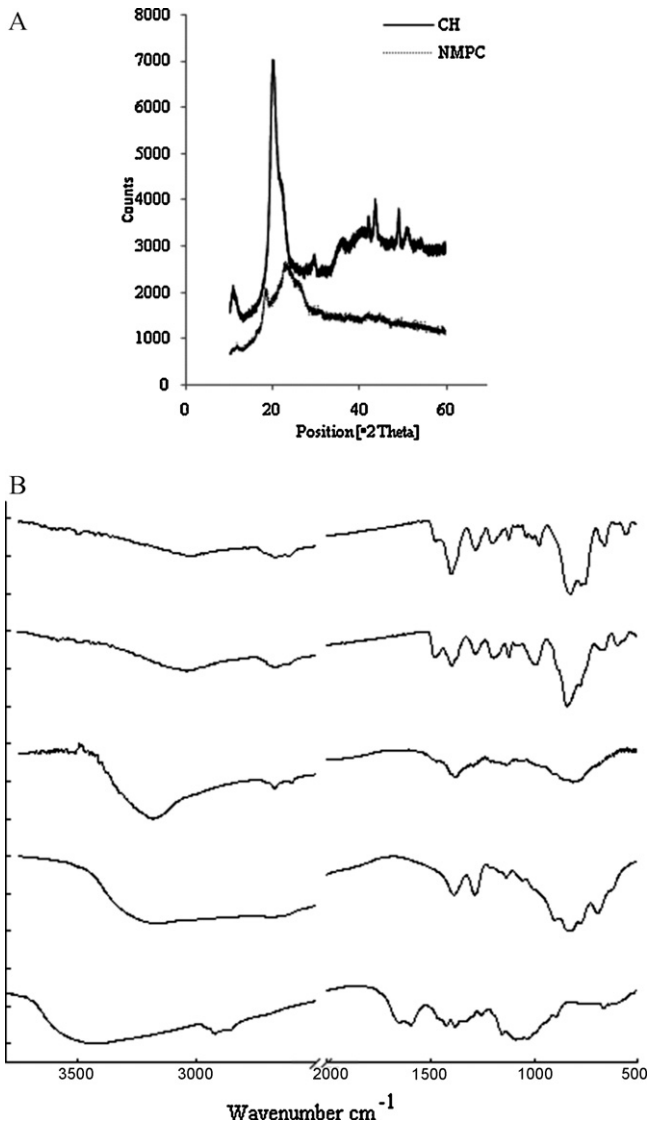

Fig. 3. (A) XRD patterns of chitosan and NMPC and (B) chemical group identification by FTIR spectrographs for (from bottom to top): chitosan (CH), N-methylene phosphonic chitosan (NMPC), NMPC–genipin gels, as spun NMPC/PVA blend nanofibers and crosslinked NMPC/PVA blend nanofibers.

low, it can be seen that major effect of PVA is by decreasing the solution conductivity and surface tension without reducing solution viscosity thus creating an optimum balance between all the parameters which determine formation of electrospun nanofibers. Resultant nanofibers were uniform and had a mean diameter of 210 ± 43 nm as calculated by 'Image J' over 100 random points. These fibers were produced at the following electrospinning conditions – 18 kV applied voltage, 10 cm tip to collector distance and solution flow rate of 5 μl/min. The nanofibers of blended polymers were crosslinked with glutaraldehyde solutions as this is one of the preferred method reported for many cell culture studies with PVA nanofibers and membranes (Zhou et al., 2008). This step is essential to render water stability to the nanofibers as otherwise due to large surface area, nanofibers dissolve quickly in cell culture media. After crosslinking, the integrity of nanofibrous architecture was found to be retained (figure not shown). Crosslinking also ensured that nanofibers maintained integrity during sterilization in 70% ethanol and after prolonged immersion in aqueous media pointing towards their suitability for evaluation in biomedical applications.

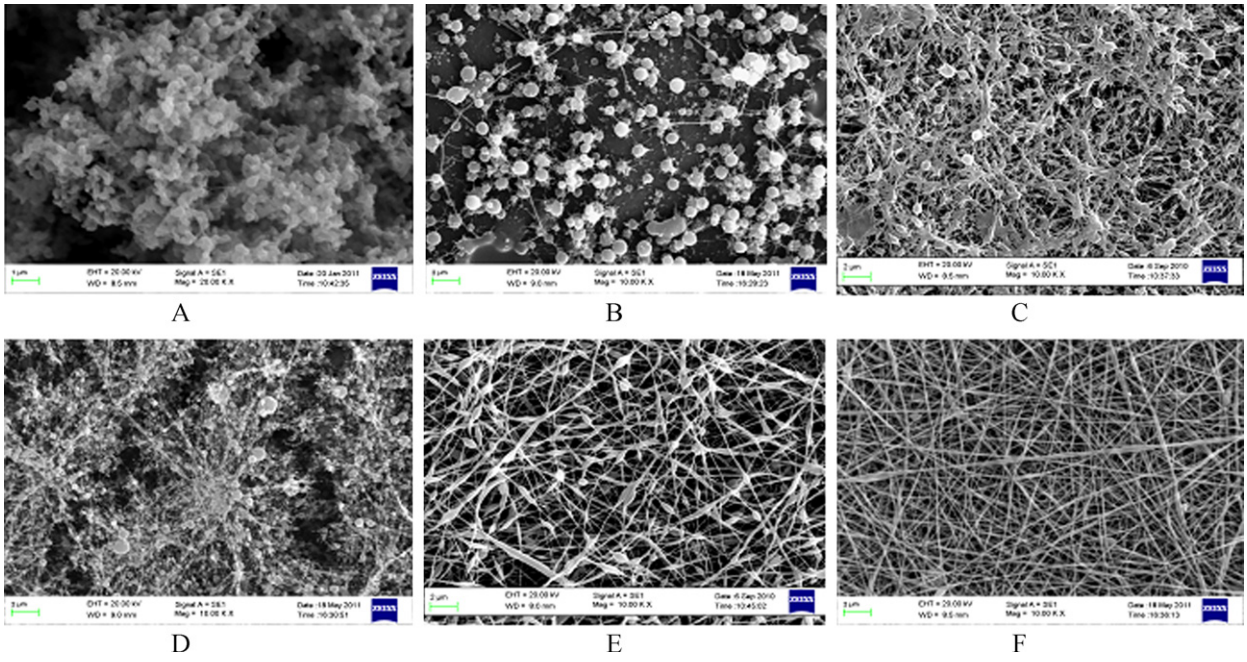

Fig. 4. Scanning electron microscopic images of as spun deposits collected after electrospinning solutions of N-methylene phosphonic chitosan and additives at fixed condition (field strength 18 kV, tip to collector distance 10 cm and flow rate 5 μL/min): (A) 4% NMPC solution in 1 M acetic acid, (B) 8% NMPC solution in 1 M acetic acid, (C) NMPC + Triton X in 1 M acetic acid, (D) NMPC + Triton X + 0.5 M NaCl, (E) NMPC + PVA (3:1) and (F) NMPC + PVA (01.5:1).

3.4. Functional group characterization of NMPC scaffolds

Analysis of the FTIR spectrum depicted in Fig. 3B elucidates the functional group differences between chitosan, phosphorylated chitosan, genipin crosslinked hydrogels and electrospun NMPC blend mats. As received chitosan exhibited a broad peak in region 3600–3000 cm^{-1} (–OH and $–NH_2$)vibrations, and three amide peaks at 1647 cm^{-1} (amide I), 1595 cm^{-1} (amide II) and 1381 cm^{-1} (amide III) of the polymer. In the phosphorylated product, broadening and weakening of $–OH/–NH_2$ compared to methylene stretches of 2800–2900 cm^{-1} region was observed suggesting hydrogen bonds getting affected (Ramos et al., 2003). The amine deformations are shifted to lower frequencies and are split into two, namely an asymmetric 1636 cm^{-1} and symmetric 1537 cm^{-1} deformation. Apart from these, new bands are observed in 1281, 938 and 505 cm^{-1} wave numbers indicated presence of P═O, and P–OH groups. The peak at 1416 cm^{-1} was attributed to $–CH_2–$ vibrations of methylene phosphonic groups in the molecule. Moreover, the –C–O–C– stretch region in 1000–1150 cm^{-1} showed a shifting towards lower frequencies but a stronger signal due to overlapping with –C–P– absorption. Spectra of genipin crosslinked hydrogels, displayed sharp but reduced intensity at 3600–3200 cm^{-1}, and increased intensity in the C–N stretch (aliphatic amines from 1250 to 1020 cm^{-1}) corresponding to the covalent bond formation during reaction of genipin with NMPC. Moreover, at 2850 cm^{-1} a sharp peak is observed which was due to increase in number of methyl groups The electrospun nanofibers of PVA/NMPC blends contained signals characteristics of both the polymers, e.g. the 1731 cm^{-1} of PVA, 1646 cm^{-1}, 1626 cm^{-1}, 1536 cm^{-1} and 943 cm^{-1} peak of NMPC in the blend nanofibers. In the crosslinked nanofibers, changes in spectral bands observed were the broadening in the 1710–1600 cm^{-1} region compared to uncrosslinked blended fibers, increased absorbance of 2850 cm^{-1} corresponding to aldehyde vibrations and broadening at –N–C– absorption region overlapping with the –C–O–C– peaks but preserving the phosphate peaks.

3.5. Biomineralization of NMPC based scaffolds

The ability of NMPC to support biomineralization was evaluated by immersion of the genipin crosslinked gels and electrospun nanofibers in SBF. SBF is a supersaturated solution with respect to calcium and phosphate ions. In the presence of nucleation sites on the matrix, clusters of calcium salt form and result in mineralization of the matrix. With respect to bone tissue engineering and bone graft materials, formation of such calcium phosphate layers on the grafts are deemed to be a prerequisite for osteoconductivity (Cornell, 1999). The calcium phosphate mineralization also results in formation of organic–inorganic hybrids typical of native

Table 1
Physicochemical property of various NMPC solutions and their effect on electrospinning.

Polymer solution	Polymer conc. (wt%)	Solvent	pH	Conductivity (mS/cm)	Surface tension (mN/m)	Viscosity (Pa s)	Electrospinnability
Chitosan	4%	1 M AA[a]	3.1	4.71 ± 0.15	68.73 ± 0.03	1.10	Splashing
NMPC	4%	Water	2.7	1.33 ± 0.22	66.16 ± 0.13	0.19	Splasing
NMPC	4%	1 M AA	2.3	4.09 ± 0.11	58.15 ± 0.06	0.16	Nanoparticles
NMPC	8%	1 M AA	2.5	3.80 ± 0.69	62.14 ± 0.55	1.02	Splashing
NMPC + Triton X (1%)	8%	1 M AA	2.3	3.69 ± 0.54	40.69 ± 1.12	0.085	Nanoparticles
NMPC + Triton X (1%) + 0.5 M NaCl	8%	1 M AA	2.4	4.94 ± 0.21	39.16 ± 0.11	0.081	Beads
NMPC + PVA (3:1)	6%, 2%	Water	3.5	1.08 ± 0.01	50.26 ± 0.88	0.37	Beaded fibers
NMPC + PVA (1.5:1)	4.8%, 3.2%	Water	3.3	0.85 ± 0.04	45.13 ± 0.36	1.07	Perfectly defect free nanofibers

[a] Acetic acid.

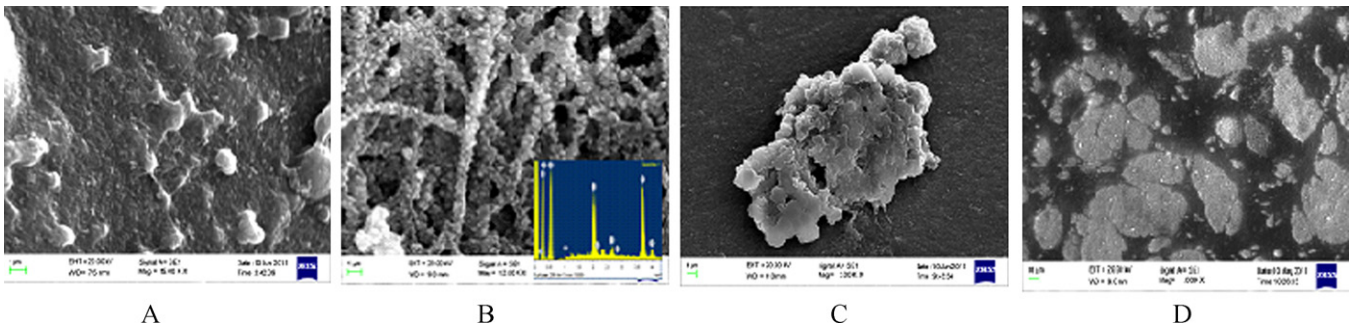

Fig. 5. Bioactivity of various NMPC scaffolds demonstrated by representative SEM graphs obtained on (A) SBF treated mineralization on PCG after 3 days, (B) incubation of NMPC-NF in SBF for 3 days (with the EDX spectra of mineral deposited *n* inset), (C) adhesion of a pre-osteoblastic cells on PCG after 24 h cell seeding, and (D) growth to full confluence of MG 63 cells on PCNF on day 7 of cell seeding. Images are acquired as part of different experiments and at different magnifications represented in the bottom panel of each image.

bone ECM. In the present work, SEM images showed that NMPC blended nanofibers were mineralized to a greater extent compared to NMPC–genipin gels (Fig. 5A). After 3 days of treatment, the nanofibrous matrix exhibited uniform and complete mineral deposition. Significant mineral deposition was also observed on gels but the deposits were not homogenous. Electrospun nanofibers offer a higher surface area and grafting of a phosphonic acid groups, known to posses chelating properties for calcium ions may be responsible for characteristics mineralization. Moreover, it was clearly visible from Fig. 5B that mineralization of nanofibers was controlled and occurred along the length of the nanofibers resulting *in situ* formation of fiber-mineral composites. On the above matrices, presence of phosphonic acid groups acted as possible sites for promoting surface-directed nucleation and subsequent mineralization. In nanofibers, the surface-area to volume ratio was very high, thus exposing more number of phosphonic acid groups as sites for nucleation. In both the gel and nanofiber, the chemical nature of deposited minerals investigated by EDX spectroscopy, were found to be apatite-like. Biomineralization of NMPC based scaffolds were supposed to render multiple advantages amenable for bone grafting viz. compressive strengths, better bone bonding ability and osteoconductivity to the scaffolds (Zhang & Zhang, 2004).

3.6. Biocompatibility and response of MG 63 cells

Biocompatibility of both NMPC–genipin gel (PCG) and NMPC/PVA blend nanofibrous (PCNF) scaffolds were evaluated and compared *in vitro* conditions after culturing with MG 63 cells, taking tissue culture plate as control (TCP). MTT assay was performed on days 1 (12 h), 3 and 7 of cell seeding to monitor cellular viability. MTT assay results showed 1.92×10^5, 2.18×10^5 and 2.49×10^5 viable cells on PCG, PCNF and TCP substrates respectively after 12 h of cell seeding. This showed that adhesion efficiency on PCNF was 132% and significantly higher compared to the PCG gels ($p < 0.05$). A significantly higher number of cells were observed on PCG on day 7 compared to day 3 of incubation indicating the compatibility of PCG to support cellular proliferation. On subsequent days of cell culture, in between PCG and PCNF, cellular activity remained higher on the PCNF surfaces for all the 7 days of culturing. These observations revealed a greater potential of PCNF to support cellular proliferation *in vitro* compared to PCG (Fig. 6A). Further, fluorescence microscopic staining by rhodamine–phalloidin for cytoskeletal F-actin filaments and by Hoechst for cell nuclei were used to visualize the cellular adhesion on NMPC matrices. As represented in Fig. 7A and B, polygonal morphology of cells and presence of well spread cytoskeletal filaments were observed on PCNF compared to PCG. In the later, cellular processes remained confined and accumulated in island-like area and cells exhibited more of a clustered appearance. In conjunction with the results of MTT assay, it can be concluded that PCNF matrixes support a greater number of cellular adhesion, cell–cell contacts and proliferation compared to PCG. Though cells on PCG also proliferated well, they adopted a different morphology. This may be attributed to the fact that PCNF presents a surface to the cell which contains architectural dimensions very similar to dimensions of filopodia like filaments responsible for cell–cell and cell–matrix attachment demonstrating the advantages of nanofibers for tissue regeneration applications over hydrogels. After one week of culturing, the electrospun matrixes were found to be confluent with MG 63 cells now giving rise to a cell-scaffold construct under SEM (Fig. 5D).

Osteoinductivity of PCG and PCNF was assessed by alkaline phosphatase activity as an early marker of osteogenic phenotype in addition to cellular calcium content deposited by proliferating cells on the matrix (Wang et al., 2011). Till day 3, there was no significant difference in ALP activity amongst the cells proliferating on PCG, PCNF and TCP. However, on day 7 significantly higher

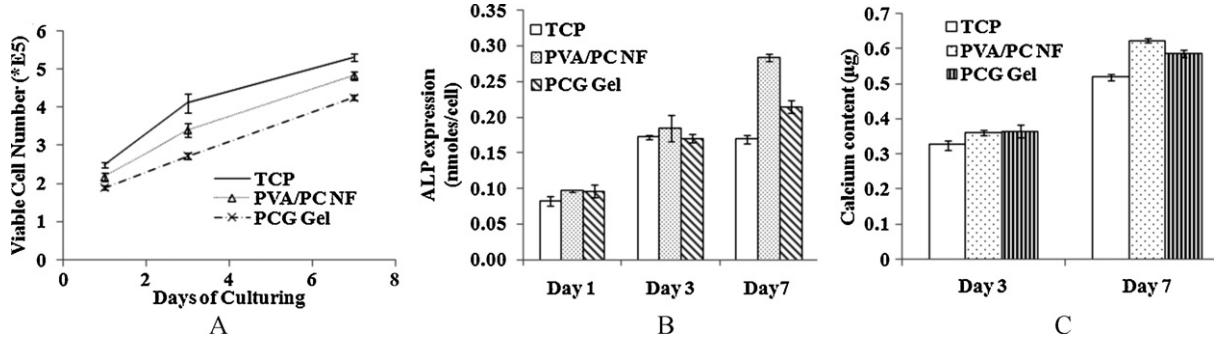

Fig. 6. Biocompatibility of NMPC hydrogels and NMPC/PVA nanofibers as evaluated by (A) viable cell number measured by MTT assay for proliferation, (B) expression of alkaline phosphatase as early phenotypic marker of osteogenic differentiation and differentiation of MG 63 cells and (C) determination of total calcium content in each scaffolds normalized for the total number of cells.

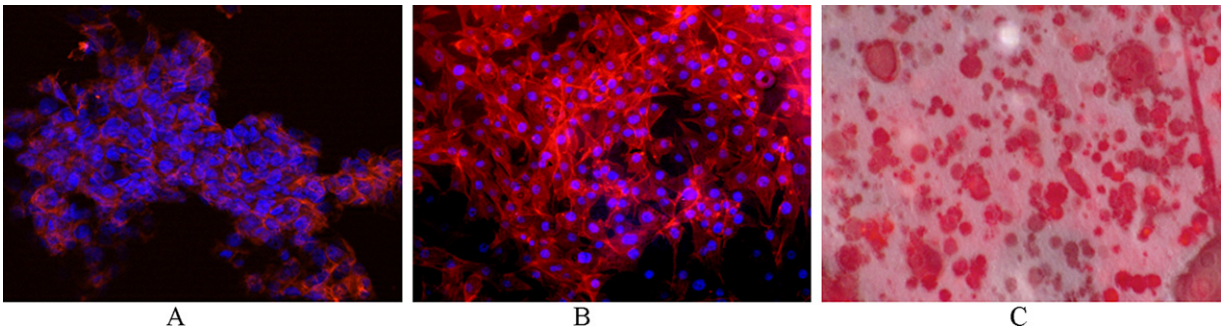

Fig. 7. Visualization of cellular activity on NMPC based scaffolds by rhodamine-Hoescht staining on (A) PCG after 5 days, (B) PCNF after 5 days and (C) Alizarin red S staining on PCNF after 7 days of MG 63 cell culture.

(1.68 times) levels of ALP activity were detected on PCNF scaffolds compared to both PCG and TCP. On PCG, cells exhibited 117% higher ALP activity compared to TCP on day 7 (Fig. 6B). Results of calcium content depicted in Fig. 6C and also revealed significantly higher calcium levels deposited by MG 63 cells in the order of PCNF (0.062 μg) > PCG (0.058 μg) > TCP (0.051 μg). Phosphorylated chitosan is reported to induce osteoblastic differentiation and this study further reinforces the applicability of a phosphorylated chitosan based scaffold in yielding osteoconductive and osteoinductive matrices with potential to serve as grafts for bone regeneration (Venkatesan, Pangestuti, Qian, Ryu, & Kim, 2010).

In summary, it can be conclusively stated that NMPC based matrices have potential to significantly drive human pre-osteoblasts like MG 63 cells towards maturation and provide good substrate for cellular adherence and proliferation. The novel scaffolds developed in this study pave the way for further fabrication of cell-scaffold constructs with osteogenic stem cells for end-use applications in bone tissue engineering.

Acknowledgements

Authors acknowledge the Mr. Goutam Thakur for providing genipin samples and the help of Mr. Nantu Dogra of School of Medical Science and Technology. Financial support from Department of Science and Technology, Government of India is acknowledged.

References

Alves, N. M., & Mano, J. F. (2008). Chitosan derivatives obtained by chemical modifications for biomedical and environmental applications. *International Journal of Biological Macromolecules*, *43*(5), 401–414.

Amaral, I. F., Granja, P. L., & Barbosa, M. A. (2005). Chemical modification of chitosan by phosphorylation: An XPS, FT-IR and SEM study. *Journal of Biomaterials Science Polymer Edition*, *16*(12), 1575–1593.

Angammana, C. J., & Jayaram, S. H. (2008). Analysis of the effects of solution conductivity on electro-spinning process and fiber morphology. In *Industry applications society annual meeting, IAS'08* (pp. 1–4). IEEE.

Bhattarai, N., Edmondson, D., Veiseh, O., Matsen, F. A., & Zhang, M. (2005). Electrospun chitosan-based nanofibers and their cellular compatibility. *Biomaterials*, *26*, 6176–6184.

Chakraborty, S., Liao, I.-C., Adler, A., & Leong, K. W. (2009). Electrohydrodynamics: A facile technique to fabricate drug delivery systems. *Advanced Drug Delivery Reviews*, *61*(12), 1043–1054.

Cornell, C. N. (1999). Osteoconductive materials and their role as substitutes for autogenous bone grafts. *Orthopaedic Clinics North America*, *30*(4), 591–598.

George, A., & Veis, A. (2008). Phosphorylated proteins and control over apatite nucleation, crystal growth and inhibition. *Chemical Reviews*, *108*, 4670–4693.

Ilyina, A. V., Varlamov, V. P., Tikhonov, V. E., Yamskov, I. A., & Davankov, V. A. (1994). One-step isolation of a chitinase by affinity chromatography of the chitinolytic enzyme complex produced by *Streptomyces kurssanovii*. *Biotechnology and Applied Biochemistry*, *19*(2), 199–207.

Jung, B.-O, Na, J., & Kim, C. H. (2007). Synthesis of chitosan derivatives with anionic groups and its biocompatibility in vitro. *Journal of Industrial Engineering Chemistry*, *13*(5), 772–776.

Kim, I.-Y., Seo, S.-J., Moon, H.-S., Yoo, M.-K., Park, I.-Y., Kim, B.-C., et al. (2008). Chitosan and its derivatives for tissue engineering applications. *Biotechnology Advances*, *26*(1), 1–21.

Kokubo, T., & Takadama, H. (2006). How useful is SBF in predicting in vivo bone bioactivity? *Biomaterials*, *27*(15), 2907–2975.

Kretlow, J. D., & Mikos, A. G. (2007). Mineralization of synthetic polymer scaffolds for bone tissue engineering. *Tissue Engineering*, *13*(5), 927–938.

Lebouc, F., Dez, I., & Madec, P.-J. (2005). NMR study of the phosphonomethylation reaction on chitosan. *Polymer*, *46*, 319–325.

Lennon, D. P., & Caplan, A. I. (2006). Mesenchymal stem cells for tissue engineering. In G. Vunjak-Novakovic, & R. I. Freshney (Eds.), *Culture of cells for tissue engineering* (pp. 23–61). New Delhi: Wiley India Pvt Ltd.

López-Pérez, P. M., da Silva, R. M. P., Serra, C., Pashkuleva, I., & Reis, R. L. (2010). Surface phosphorylation of chitosan significantly improves osteoblast cell viability, attachment and proliferation. *Journal of Materials Chemistry*, *20*, 483–491.

Madurantakam, P. A, Rodriguez, I. A., Cost, C. P., Viswanathan, R., Simpson, D. G., Beckman, M. J., et al. (2009). Multiple factor interactions in biomimetic mineralization of electrospun scaffolds. *Biomaterials*, *30*(29), 5456–5464.

Matevosyan, G. L., Yukha, Y. S., & Zavlin, P. M. (2003). Phosphorylation of chitosan. *Russian Journal General Chemistry*, *73*(11), 1725–1730.

Moedritzer, K., & Irani, R. R. (1966). The direct synthesis of α-aminomethylphosphonic acids. Mannich-type reactions with orthophosphorous acid. *Journal of Organic Chemistry*, *31*(5), 1603–1607.

Moura, M. J., Figueiredo, M. M., & Gil, M. H. (2007). Rheological study of genipin cross-linked chitosan hydrogels. *Biomacromolecules*, *8*, 3823–3829.

Muzzarelli, R. A. A. (2009). Genipin-crosslinked chitosan hydrogels as biomedical and pharmaceutical aids. *Carbohydrate Polymers*, *77*(1), 1–9.

Nishi, N., Ebina, A., Nishimura, S.-i., Tsutsumi, A., Hasegawa, O., & Tokura, S. (1986). Highly phosphorylated derivatives of chitin, partially deacetylated chitin and chitosan as new functional polymers: Preparation and characterization. *International Journal of Biological Macromolecules*, *8*(5), 311–317.

Ohkawa, K., Cha, D., Kim, H., Nishida, A., & Yamamoto, H. (2004). Electrospinning of chitosan. *Macromolecular Rapid Communications*, *25*, 1600–1605.

Orban, J. M., Marra, K. G., & Hollinger, J. O. (2002). Composition options for tissue-engineered bone. *Tissue Engineering*, *8*, 529–539.

Pramanik, N., Mishra, D., Banerjee, I., Maiti, T. K., Bhargava, P., & Pramanik, P. (2009). Chemical synthesis, characterization, and biocompatibility study of hydroxyapatite/chitosan phosphate nanocomposite for bone tissue engineering applications. *International Journal of Biomaterials*, doi:10.1155/2009/512417

Ramos, V. M., Rodríguez, M. S., Agulló, E., Rodríguez, N. M., & Heras, A. (2002). Chitosan with phosphonic and carboxylic group: new multidentate ligands. *International Journal of Polymeric Materials*, *51*(8), 711–720.

Ramos, V. M., Rodríguez, N. M., Diaz, M. F., Rodríguez, M. S., Heras, A., & Agulló, E. (2003). N-methylene phosphonic chitosan. Effect of preparation methods on its properties. *Carbohydrate Polymers*, *52*, 39–46.

Ramos, V. M., Rodríguez, N. M., Henning, I., Díaz, M. F., Monachesi, M. P., Rodríguez, M. S., et al. (2006). Poly(ethylene glycol)-crosslinked N-methylene phosphonic chitosan. Preparation and characterization. *Carbohydrate Polymers*, *64*(2), 328–336.

Seol, Y.-J., Lee, J.-Y., Park, Y.-J., Lee, Y.-M., Ku, Y., Rhyu, I.-C., et al. (2004). Chitosan sponges as tissue engineering scaffolds for bone formation. *Biotechnology Letters*, *26*(13), 1037–1041.

Song, J., Malathong, V., & Bertozzi, C. R. (2005). Mineralization of synthetic polymer scaffolds: A bottom-up approach for the development of artificial bone. *Journal of American Chemical Society*, *127*(10), 3366–3372.

Stevens, M. (2008). Biomaterials for bone tissue engineering. *Materials Today*, *11*(5), 18–25.

Sugihara, J., Imamura, T., Yanase, T., Yamada, H., & Imoto, T. (1982). Separation of peptides by cellulose-phosphate chromatography for identification of a hemoglobin variant. *Journal of Chromatography*, *229*, 193.

Tang, T., Zhang, G., Lau, C. P., Zheng, L. Z., Xie, X. H., Wang, X. L., et al. (2011). Effect of water-soluble P-chitosan and S-chitosan on human primary osteoblasts and giant cell tumor of bone stromal cells. *Biomedical Materials*, *6*, 1–9.

Uchino, T., Kamitakahara, M., Otsuka, M., & Ohtsuki, C. (2010). Hydroxyapatite-forming capability and mechanical properties of organic–inorganic hybrids and

α-tricalcium phosphate porous bodies. *Journal of Ceramic Society of Japan*, *118*(1), 57–61.

Venkatesan, J., Pangestuti, R., Qian, Z.-J., Ryu, B., & Kim, S.-K. (2010). Biocompatibility and alkaline phosphatase activity of phosphorylated chitooligosaccharides on the osteosarcoma MG63 cell line. *Journal of Functional Biomaterials*, *1*, 3–13.

Wang, G., Zheng, L., Zhao, H., Miao, J., Sun, C., Ren, N., et al. (2011). In vitro assessment of the differentiation potential of bone marrow-derived mesenchymal stem cells on genipin–chitosan conjugation scaffold with surface hydroxyapatite nanostructure for bone tissue engineering. *Tissue Engineering Part A*, *17*(9–10), 1341–1351.

Xu, Z., Neoh, K. G., Lin, C. C., & Kishen, A. (2011). Biomimetic deposition of calcium phosphate minerals on the surface of partially demineralized dentine modified with phosphorylated chitosan. *Journal of Biomedical Materials Research Part B: Applied Biomaterials*, *98B*(1), 150–159.

Yin, Y. J., Luo, X. Y., Cui, J. F., Wang, C. Y., Guo, X. M., & Yao, K. D. (2004). A study on biomineralization behavior of N-methylene phosphochitosan scaffolds. *Macromolecular Biosciences*, *4*(10), 971–977.

Zhang, Y., & Zhang, M. (2004). Cell growth and function on calcium phosphate reinforced chitosan scaffolds. *Journal of Materials Science: Materials in Medicine*, *15*, 255–260.

Zhou, Y., Yang, D., Chen, X., Xu, Q., Lu, F., & Nie, J. (2008). Electrospun water-soluble carboxyethyl chitosan/poly(vinyl alcohol) nanofibrous membrane as potential wound dressing for skin regeneration. *Biomacromolecules*, *9*, 349–354.

Zhu, D., Yao, K., Bo, J., Zhang, H., Liu, L., Dong, X., et al. (2010). Hydrophilic/lipophilic N-methylene phosphonic chitosan as a promising non-viral vector for gene delivery. *Journal of Materials Science: Materials in Medicine*, *21*, 223–229.

Zhu, Y., Wang, X., Cui, F. Z., Feng, Q. L., & Groot, K. d. (2003). In vitro cytocompatibility and osteoinduction of phosphorylated chitosan with osteoblasts. *Journal of Bioactive and Compatible Polymers*, *18*(5), 375–390.